Available online at www.sciencedirect.com
ScienceDirect
Biochimica et Biophysica Acta 1757 (2006) 1084–1095
BIOCHIMICA ET BIOPHYSICA ACTA
BBA
www.elsevier.com/locate/bbabio

Review

The menaquinol-oxidizing cytochrome *bc* complex from *Thermus thermophilus*: Protein domains and subunits

Daniela Mooser [a,*], Oliver Maneg [a,b], Fraser MacMillan [c], Francesco Malatesta [d], Tewfik Soulimane [e], Bernd Ludwig [a]

[a] *Molekulare Genetik, Institut für Biochemie, Biozentrum der J. W. Goethe-Universität, 60439 Frankfurt am Main, Germany*
[b] *Sanofi-Aventis Deutschland GmbH, Industriepark Höchst H780, 65926 Frankfurt am Main, Germany*
[c] *Institut für Physikalische und Theoretische Chemie, J. W. Goethe-Universität, 60439 Frankfurt am Main, Germany*
[d] *Department of Pure and Applied Biology, University of L'Aquila, I-67010 L'Aquila, Italy*
[e] *College of Science and MSSI, University of Limerick, Ireland*

Received 17 March 2006; received in revised form 27 April 2006; accepted 23 May 2006
Available online 27 May 2006

Abstract

A recently resolved respiratory complex III, isolated from the extreme thermophile *Thermus thermophilus*, is discussed in terms of cofactor and subunit composition, and with respect to the origin of its protein modules. The four polypeptides, encoded by a single operon, share general homologies to canonical complexes both of the *bc* and b_6f type, but exhibit some unexpected features as well. Evidence for high thermostability of the isolated protein and for its quinol substrate specificity is derived from EPR and kinetic measurements. A functional integration of this complex into an aerobic electron transfer scheme, connecting known dehydrogenase activities to the terminal oxidase branches of *Thermus* is outlined, as well as the specific principles of redox protein interactions prevailing at high temperature. Findings from this enzyme are linked to present knowledge on other menaquinol oxidizing *bc* complexes.

Keywords: *Thermus thermophilus*; Respiratory chain; Cytochrome *bc*; Complex III; Menaquinone; EPR; Electron transfer; Stopped flow kinetic

1. Introduction

The attention to thermophilic organisms has recently been spurred for several reasons. From a biotechnological point of view, their heat-tolerant enzymes are of considerable interest, both for a wide array of industrial processes, as well as for analytical and methodological purposes such as PCR, where catalysts should sustain automated procedures at elevated temperatures for a prolonged time. Extended thermal stability of purified protein components and complexes derived from these organisms has also been successfully exploited in basic research for structure determinations, along with the attempt to solve the challenging question of the underlying principles of thermostability in such macromolecules (see, e.g., [1]).

From an evolutionary perspective, thermostability may provide an initial clue for a present-day niche situation for this trait of organisms reflecting early conditions and forms of life on earth [2]. These initial assumptions have been corroborated by analyzing the genealogy of thermophilic isolates, with many of them being deeply rooted in the evolutionary tree. Such views may now be further substantiated by solid information obtained from recent genome sequencing projects of both eubacterial and archaeal thermophiles (see below), and allow a differentiation from lateral gene transfer events, additionally shaping genomes and their gene products (see, e.g., [3]).

Also with the endosymbiotic progenitor relationship of bacteria with present-day mitochondria in mind, these

Abbreviations: ET, electron transfer; aa, amino acid; ORF, open reading frame; RBS, ribosome binding site; I, ionic strength; MALDI, matrix-assisted laser desorption ionization; MS, mass spectrometry; TMPD, tetramethyl-p-phenylendiamin; NDH-1, NADH:quinone oxidoreductase-1 (energy transducing); NDH-2, NADH:quinone oxidoreductase-2; MK-8, menaquinone-8; SDS, sodium dodecyl sulfate; FeS, iron–sulfur center; E_0', standard redox potential; CD, circular dichroism; EPR, Electron paramagnetic resonance

* Corresponding author.
E-mail address: d.mooser@em.uni-frankfurt.de (D. Mooser).

0005-2728/$ - see front matter © 2006 Elsevier B.V. All rights reserved.
doi: 10.1016/j.bbabio.2006.05.033

evolutionary relicts may provide molecular clocks for phylogenetic development [4]. In adapting from thermo- to mesophilic and, in parallel, from poor to high oxygen level environments, these microorganisms developed specific electron transfer (ET) chains, shifting redox potentials of their redox mediators and altering their modes of interaction between redox protein complexes embedded in the membrane.

Strains of the extremely thermophilic and halotolerant *Thermus thermophilus* have first been isolated from hot springs in the early 1970s, and on phylogenetic grounds grouped into the common branch *Deinococcus–Thermus*, despite a low degree both of phenotypic consensus and of gene synteny, recently reviewed in [3]. Presently, two complete genome sequences are available for strain HB27 with its 1.9 Mb chromosome and an accompanying 0.2 Mb megaplasmid [5] and for strain HB8 [6]. Present interest from basic science, and also from biotechnology, for *Thermus* proteins ranges from DNA polymerases, even expressed to high yield in the homologous host [7], all the way to multi-subunit complexes such as ATPases [8] or ribosome complexes [9].

The ET chain components and energy transduction capacity of this thermophile has been acknowledged early-on [10] as being generally similar to that of many mesophilic organisms (see Fig. 1), with the notable exception that the only redox-active quinone present in the organism is a menaquinone moiety instead of ubiquinone [11].

Terminal oxidases have been described for *Thermus* as early as 1980 when a heme *c* containing aa_3 complex was identified [12,13] and later shown (i) to receive electrons directly from a soluble c_{552} (but see below), (ii) to act as a proton pump [14,15], and (iii) its canonical subunit II covalently fused with a C-terminal heme *c* domain [16]. Unlike this oxidase which is expressed mainly under aerobic conditions, a second terminal oxidase (Fig. 1) synthesized mostly under low oxygen tension has been isolated [17]. This ba_3-type oxidase was later crystallized and its structure solved [18]; being a more distant member of the large family of terminal oxidases [19], it lacks some of the canonical amino acid "signatures" defining proton channels and electron pathways, and was shown to translocate protons only with a diminished stoichiometry on reconstitution [20].

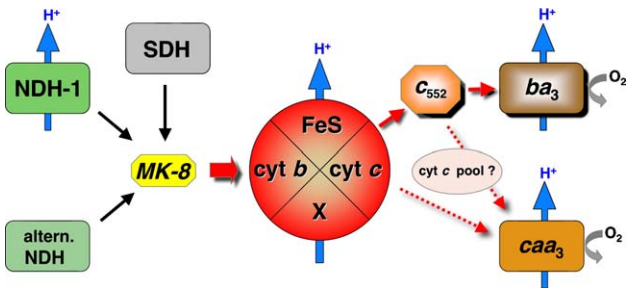

Fig. 1. Schematic minimal scheme of the aerobic electron transport chain in *T. thermophilus*, highlighting the central role for the cytochrome *bc* complex (in red) and its presumed interactions with known redox components. NDH-1, NADH:quinone oxidoreductase; SDH, succinate:quinone oxidoreductase; MK-8, menaquinone-8; shaded components, structures determined by X-ray crystallography; blue vertical arrows: presumed or confirmed energy transduction sites; dotted arrows, hypothetical ET routes; for further explanations, see text.

Cytochrome c_{552}, a soluble mono-heme protein identified as early as 1977 [21], has later been crystallized, its structure solved to high resolution, and extensively discussed for the structural basis of its thermostability [22]. This cytochrome (Fig. 1) reacts readily and specifically with the isolated ba_3 oxidase [23], as well as with the soluble Cu_A fragment derived from it [24] when studied by a stopped-flow approach [25]. A careful kinetic analysis confirms that these *Thermus* components interact mainly via hydrophobic forces, in contrast to the situation in mitochondria and many bacterial ET chains where oppositely charged surfaces on both partner proteins govern their long-range interaction [26]. Along with this notion, it was shown that no ET cross-reactivity between the mitochondrial cytochrome *c* and the *Thermus* ba_3 oxidase exists [23]. There is conflicting evidence at present as to whether the c_{552} also serves as the electron donor to the caa_3 oxidase, see below.

On the ET chain entry level, several different NADH dehydrogenases have been described for *Thermus*. NDH-1 resembles the mitochondrial complex I in its general energy-transducing capability, but consists of only 14 subunits [27,28], thus making it a suitable model system for the far more complex mitochondrial enzyme. The structure of the hydrophilic part of this respiratory enzyme, containing all the FeS redox centers, has recently been solved by X-ray crystallography [29,30]. On the contrary, the other, quinone-dependent NDH-2 is non-energy transducing, and consists of only a single polypeptide lacking any FeS cofactors [27], while yet another, even less specific NADH dehydrogenase activity bypasses the quinone pool, catalyzing the formation of hydrogen peroxide [31,32]. Electrons also reach the menaquinone-8 pool from the succinate dehydrogenase complex [33].

It is interesting to note (recently reviewed in [34]) that one of the two *T. thermophilus* strains, HB8, is endowed with a conjugative plasmid allowing anaerobic growth on nitrate; it encodes, among others, a nitrate reductase complex and an additional, nitrate-specific heterotetrameric NADH dehydrogenase of unusual subunit composition.

A complex III activity, central to the ET chain of *Thermus* by linking the dehydrogenase activities with the terminal oxidase branches, has recently been identified [35]; for a detailed description, see below. Early evidence had already pointed to a potential complex III component, a soluble fragment of a Rieske FeS protein, which was characterized extensively in terms of its structure and function [36–39].

To date comprehensive information on purified, naphtho-quinol-oxidizing *bc* complexes has been scarce. A complex resembling the typical proteobacterial bc_1 complexes in subunit and cofactor composition (for recent reviews, see [5,40–42]) was isolated from *Aquifex aeolicus*, a hyperthermophilic bacterium, consisting of a 40 kDa cytochrome *b* (E_0'=−60/+160 mV for b_L and b_H, respectively), a 25 kDa cytochrome c_1 (+160 mV), and a 21 kDa FeS subunit (+210 mV for a soluble form of the heterologously expressed protein). While these electrochemical data are in line with the low redox potential of

the naphthoquinol oxidized by this enzyme, a phylogenetic analysis together with the contrasting fact that the cytochrome *c* subunit represents a monoheme protein, suggest that the *Aquifex* genes have been acquired from a highly distant proteobacterial donor in a lateral gene transfer scenario [43].

A thermostable, four-subunit "bc_1" complex was isolated from the bacillus PS3 (related to *B. stearothermophilus*; [44]), resembling in several aspects a chloroplast b_6f complex with low redox potential components (−190 and −160 mV for the two *b*-hemes, but 200 mV for the *c/f*-type cytochrome) and a typical Rieske EPR signature with an E_0' of 165 mV at pH 7 [45]. A stable association of this complex III with its terminal oxidase, yielding a seven-subunit supercomplex, has been reported under certain solubilization conditions [44].

Another bacillus species, *B. subtilis*, has been analyzed mostly on genetic grounds and in intact membranes for the presence of a menaquinol:cytochrome *c* reductase activity [46]. The corresponding tricistronic operon encodes a Rieske FeS subunit, a 224 amino acid cytochrome *b* (corresponding to the larger fragment of the split b_6f version, see [41]), and an unusual third gene product consisting of the small *b* fragment of 170 residues fused to a *c*-heme domain of 86 residues strongly resembling the soluble cytochrome c_{550} sequence. This has been cited as an interesting example for "domain swapping", making use of a *c*-cytochrome sequence unrelated to any of the canonical "c_1" nor "*f*" cytochrome domains found as subunits in typical complexes III (see also below).

A menaquinol-dependent bc_1 complex from the aerobic mesophile *Corynebacterium glutamicum* can be isolated in the form of a quinol oxidase supercomplex; its cytochrome *c* carries two hemes, presumably to mediate direct ET to the aa_3-type terminal oxidase branch [47]; in a related bacterium, *Rhodococcus rhodochrous*, a comparable situation is met for its di-heme *c*-subunit [48]. An unusual multiheme *bc* complex from *Rhodothermus marinus*, a thermohalophilic aerobe, was reported to lack a Rieske-type FeS center [49].

2. The *Thermus thermophilus bc* complex—genetic framework and functional setup

2.1. Four genes are organized in an operon structure

Originally applying the Rieske consensus motif information in a tBLASTn search [50] on preliminary genomic sequence information (Genomics Laboratory Göttigen, Germany; now published in [5]), one of the two resulting hits could be clearly assigned to the Rieske center domain, characterized extensively earlier as a soluble fragment [36,37]. Analyzing its neighbouring sequences, a chromosomal gene locus termed *fbc*CXFB became obvious [35]. This operon-like structure of 3.1 kb with a GC-content of 69% encodes four consecutive open reading frames (ORF) (Fig. 2B), spaced by only 8–10 bp each of noncoding sequence. All four genes use ATG as the start codon,

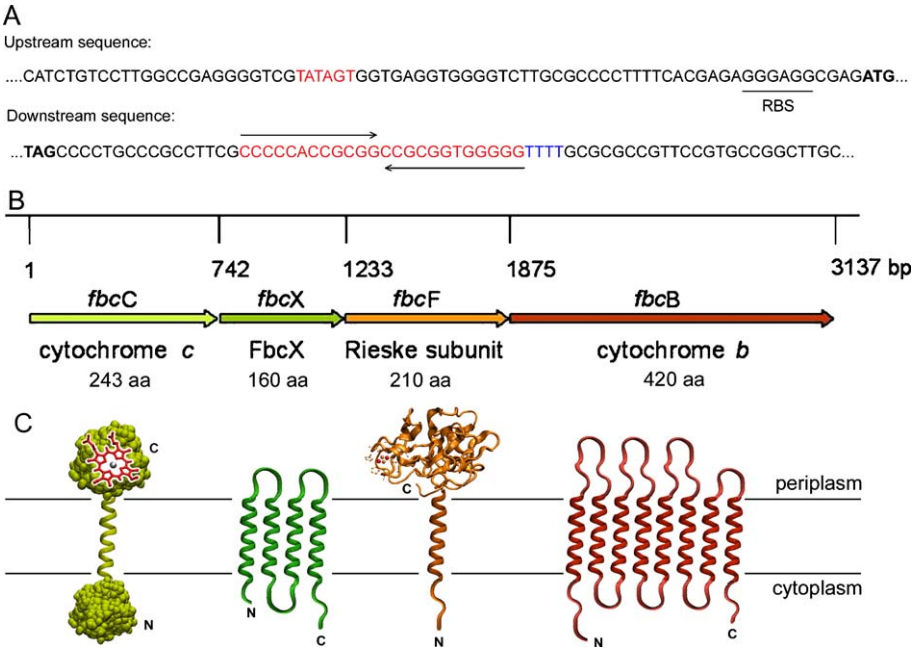

Fig. 2. Genetic organization of the *fbc* operon and membrane topology prediction of the four gene products. (A) Sequence elements up- and downstream of the *fbc* operon. A typical TATA box (in red) is found in front of the first ATG (in bold) of the first gene, preceded by a ribosome binding site (RBS). In the sequence downstream of the stop codon (TAG in bold) of the last gene of the operon, a transcription termination loop is indicated by the two arrows flanking the 24 bp palindromic sequence (highlighted in red) followed by four thymidines. (B) Operon structure and gene organization of the *fbc*CXFB operon. Numbers denote start positions of the coding sequences of all four genes, and the stop position of the cytochrome *b* gene. Below each gene, the expected number of amino acids (aa) of the products are listed. (C) Domain topology predictions for the four *T. thermophilus bc* complex subunits in relation to the membrane, as deduced from DAS hydropathy plots (see also Fig. 4) as well as from sequence homology; for details, see text. Domains are depicted purely schematic, with the exception of the hydrophilic FeS domain characterized structurally as a soluble fragment [38].

while stop codons are diverse (TAA, TGA, TAG). A ribosome binding site (RBS) can be identified 4–7 bp upstream of each individual start codon. The 5′-region features a typical σ^{70} prokaryotic TATA box (see Fig. 2A) 44 bp upstream of the start codon of the first gene. At a distance of 16 bp downstream of the last stop codon, a perfect termination loop is identified (Fig. 2A), consisting of a 24 bp palindromic sequence followed by four thymidines. Altogether these features indicate a canonical prokaryotic operon resulting in a polycistronic mRNA transcript for the four coding regions.

2.2. The operon fbcCXFB encodes four proteins: functional description and topology prediction

By homology searches, three of the four hypothetical gene products are easily identified as typical *bc* components to allow unequivocal assignment of the operon products, with the exception of the second ORF (see Fig. 2B): cytochrome *c*, FbcX (see below), a Rieske $Fe_2 \cdot S_2$ protein, and cytochrome *b*. All four proteins are later shown to be integral components of the *bc* complex of *T. thermophilus*.

2.2.1. Cytochrome c

The first ORF encodes a monoheme *c*-type cytochrome of 243 aa with a calculated molecular mass of 26 kDa. A hydropathy plot (Fig. 4A), calculated by the DAS-method (Dense alignment surface) [51], suggests one hydrophobic stretch of at least 13 aa (Pos. 106–118). This putative transmembrane helix is located in the center of the polypeptide, probably creating two hydrophilic domains separated by the membrane (Fig. 2C).

The C-terminal hydrophilic domain of 124 aa comprises the typical binding motif for *c*-type hemes (Pos. 171–175, CAACH). As judged from the expected site of *c*-heme incorporation and the confirmed interaction of this domain with the periplasmic cytochrome c_{552} (see below), we propose this domain facing the periplasm (Fig. 2C).

Using a polyclonal antibody generated against the C-terminal heme domain of this protein, we confirmed the expected molecular weight of the full-length protein in native *Thermus* membranes and in the isolated complex by Western blotting. Additionally the N-terminal hydrophilic domain of around 100 aa was proven by MALDI-MS to be present in the isolated cytochrome subunit [35]. We can therefore safely exclude the possibility that this domain might serve as a signal sequence of unusual length to be cleaved off the primary translation product. Until now we have no experimental evidence as to the sidedness of this domain, but assume its cytoplasmic orientation from the clear-cut hydropathy plot (Fig. 4).

The presence of a charge transfer band of the ferricytochrome *c* at 695 nm [35] indicates that a methionine (possibly M212, see Fig. 3) can be assumed as the sixth heme ligand, classifying this protein as a *c*-type cytochrome rather than a cytochrome *f* [52].

Running a similarity search with Fasta3 (FASTA version 3 at the EBI [53]), the unexpected topology of this subunit is mirrored by the fact that no homology over the full length of the sequence is detected. Partial homologies are obvious especially for the heme containing C-terminal domain (pos. 158–243) and a central portion of the protein (pos. 58–157, see The FbcX gene product section, below), while no reasonable homology with published sequences is attributable to the first 50 residues of the hydrophilic N-terminal domain. To our surprise, the C-terminal heme domain of about 86 aa (Fig. 3A, top line) consistently aligns with portions of subunit II of mostly γ-proteobacterial caa_3 oxidases, rather than to any monoheme *c*-type sequence of known *bc* complexes. Fig. 3A presents this extensive homology between the *T. thermophilus* complex III domain (master sequence) and the five best caa_3 oxidase *c*-heme domains that are fused to the C-terminus of the typical hydrophilic Cu_A binding domain of subunit II. As can be seen, homologies extend far beyond the core heme-liganding motif (CXYCH), and cover the whole domain, leading to a sequence identity between all 6 aligned sequences of about 29% (plus another 30% in similarity).

T. thermophilus contains a caa_3 terminal oxidase as well; its *c*-domain does not show up in a standard multi-sequence alignment. However, in a side-by-side comparison allowing for the introduction of several gaps (Fig. 3B), the homology

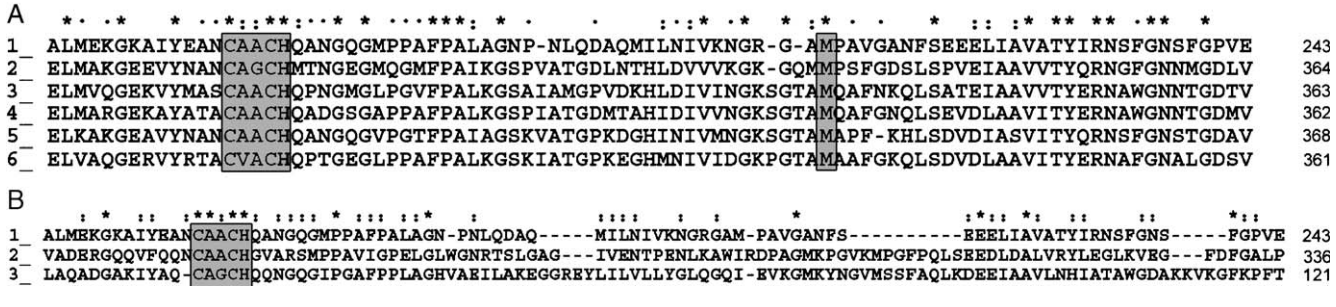

Fig. 3. Sequence comparison of the *T. thermophilus* FbcC heme *c* binding domain in a multiple sequence alignment performed with Clustal X (1.83). (A) The *T. thermophilus* cytochrome *c* subunit was analyzed with the FASTA3 [version 3 at the EBI] homology search and aligned with the 5 best hits. The 86 C-terminal amino acids constituting the *c*-heme binding domain of the *Thermus* FbcC protein are shown (line 1 A, B) with the corresponding sequences of 5 *c*-domains fused to subunit II sequences from caa_3 oxidases: line 2, *Methylococcus capsulatus*, Q60AH4; 3, *Shewanella amazonensis*, Q3QLP8; 4, *Marinobacter aquaeolei*, Q36PG5; 5, *Nitrobacter multiformis*, Q2YCN0; 6, *Azotobacter vinelandii*, Q4IZQ3. *, complete identity; :, 4 identical positions compared to the master sequence; ·, 2–3 identities respectively. (B) Sequence comparison of *T. thermophilus c*-heme domains derived from: line 1, FbcC; 2, caa_3 oxidase; 3, cytochrome c_{552}. *, full identity; :, one aa identity to the master sequence.

between both sequences becomes evident: the *Thermus* oxidase *c*-domain is considerably longer, yet extensive identity stretches are found over the whole domain. Phylogenetic and possible functional consequences will be discussed below.

2.2.2. The FbcX gene product

The second ORF encodes a highly hydrophobic protein of 17.6 kDa with 4 predicted transmembrane helices (each at least 11–20 aa in length; see Fig. 4). Based on the charge distribution argument [54], both the N- as well as the C-terminus should face the cytoplasm (see also Fig. 2C). Until now no evidence for a cofactor binding motif has arisen, and we can only speculate on the function of this protein component, as no appropriate counterpart was found among known subunits of *bc* complexes from mitochondria or bacteria. The only reasonable homology seen is that to the C-terminal part of a *Deinococcus* cytochrome c_6 (both from *D. geothermalis*, and *D. radiodurans* [55,56]). This monoheme cytochrome shows 4 transmembrane helices in a hydropathy plot, one at the N-terminus of the protein followed by a hydrophilic domain of about 150 aa carrying the heme binding motif, and three more helices at the C-terminal end (Fig. 4). Moreover there is a clear homology between the central part (pos. 58–237) of the *T. thermophilus* cytochrome *c* and the first half of the *Deinococcus* protein. Therefore it may be speculated that the phylogenetic

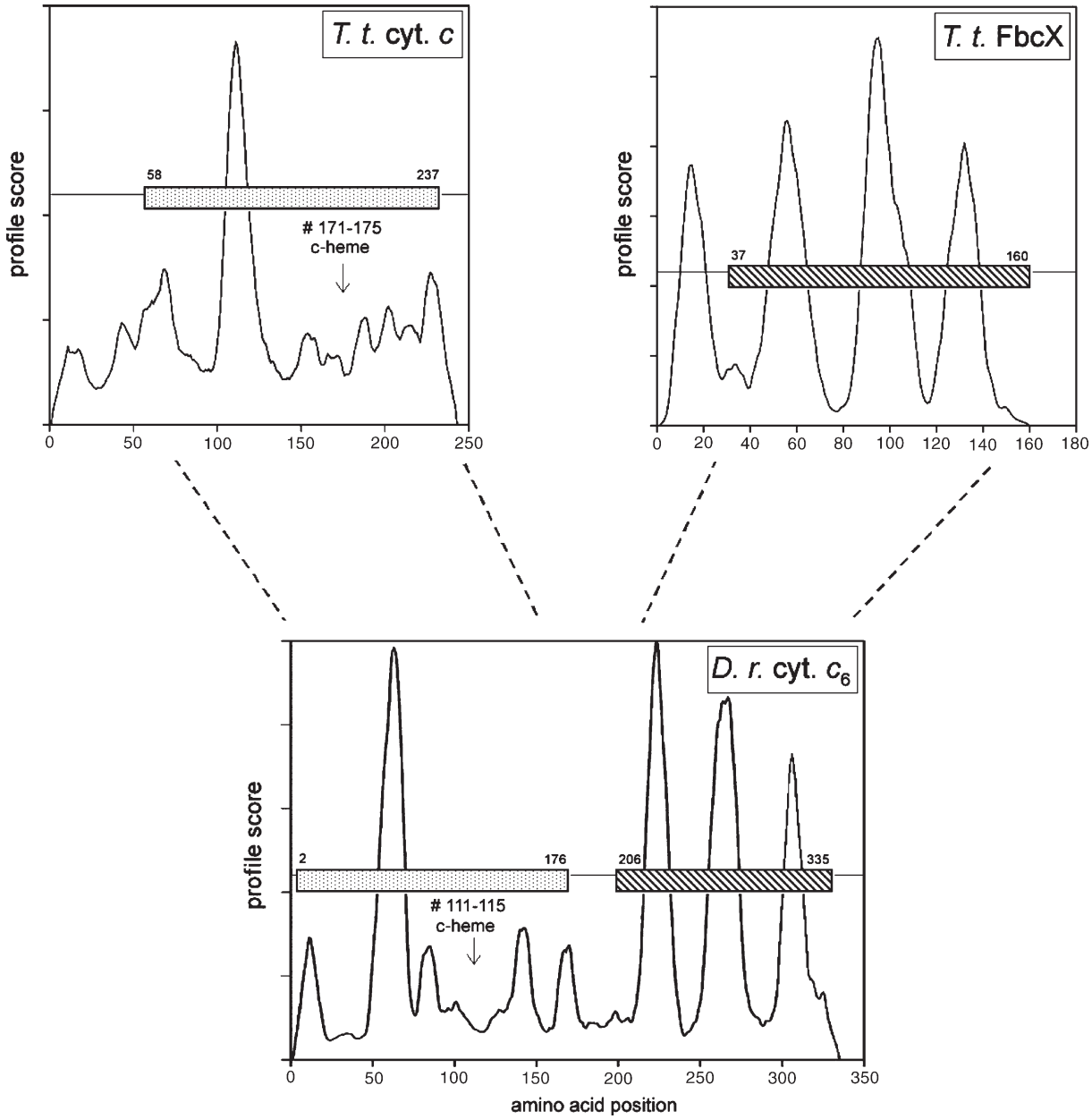

Fig. 4. Sequence homologies of the two subunits, cytochrome *c* and FbcX, with the *D. radiodurans* cytochrome c_6 [56]. Hydropathy plots calculated by the DAS method [51]. Values above threshold (strict cut off; solid line) denote presumed transmembrane helices. Differently filled bars denote sequence stretches with a high degree of identity, respectively.

origin of this additional subunit in the *T. thermophilus bc* complex may lie in a splitting or fusion event in a gene common to both bacteria.

With the two subunit sequences sharing homologies with the *D. radiodurans* c_6 sequence as outlined in Fig. 4, this "fused" polypeptide should exhibit a topology with both N- and C-termini located on the cytoplasmic side of the membrane, lending further support to the assumed orientation of both individual subunits as depicted in Fig. 2.

2.2.3. The $Fe_2 \cdot S_2$ Rieske protein

The third gene in the operon codes for a Rieske iron–sulfur protein of 22.4 kDa, consisting of a single, N-terminal hydrophobic transmembrane helix of about 13 aa and a distinct TAT-export signal sequence (SRRRLFLK, pos. 11–18; see, e.g., [57]). We identified the presence of the major part of this hydrophobic stretch in the purified protein by MALDI MS [35], and therefore, assign it a dual function, that of an export signal and a membrane anchor at the same time.

The C-terminal hydrophilic part of this protein carrying the FeS-cluster binding domain has already been expressed in *E. coli* and its crystal structure solved at high resolution [37] revealing two structural domains. The smaller one includes the highly conserved FeS-binding motif with a strong homology to known Rieske proteins. In contrast the larger domain is dominated by β-sheets forming an irregular barrel, and together with a bilobal shape of this polypeptide, it rather resembles the b_6f-type Rieske proteins.

2.2.4. Cytochrome b

The last gene in the *fbc* operon encodes the cytochrome *b* resulting in a 47.5 kDa protein. Its 420 aa are largely hydrophobic, and at least 8 transmembrane helices are predicted by a hydropathy plot [35], fully in line with 3-D structural information of complexes III from other sources. Especially the first three of the four loop structures protruding to the periplasm are largely extended (48, 53, 53 aa) but also the N-terminus is elongated as indicated schematically in Fig. 2C. Most prominent sequence identities can be assigned especially to the first half (helix 1–4) of the protein: this includes the consensus motifs for heme-*b* binding in helices II and IV.

As no third heme binding motif for a c_i heme, requiring one cysteine residue close to the N-terminus, can be identified and the protein is present in an unsplit form [58], it can be classified as a typical mitochondrial-type cytochrome *b*, although a general sequence relation to the b_6 cytochrome should be noted. In sequence alignments the highest degree of identity is again seen with the *Deinococcus* group members (45%) but only 25% to cytochrome *b* from yeast.

2.3. Experimental access to the T. thermophilus bc complex and its expression in the homologous host

To identify and biochemically characterize this *bc* complex, the entire coding region of the operon together with its presumed upstream promotor region (see above) was amplified from genomic DNA of strain HB8 (ATCC 27634), and a His-tag sequence added for expression at the C-terminus of the cytochrome *b*. This PCR amplicon was subsequently cloned into a *Thermus/E. coli* shuttle vector based on the construct pNTsp2 [35], encoding a heat-stable kanamycin resistence (HTK) gene sequence for selection at growth temperatures up to 70 °C. After electroporating this construct into *Thermus* (HB27 ATCC BAA-163), cells were grown overnight in rich medium supplemented with kanamycin.

For the isolation of the *bc* complex *Thermus* membranes were prepared and solubilized with n-decyl-β-D-maltoside. Purification was achieved on a metal affinity column followed by gel filtration; see [35] for experimental details.

The purified, His-tagged *Thermus bc* complex was analyzed by different protein chemical methods and shown to consist of all four subunits encoded in the *fbc* operon in an SDS-PAGE analysis (Fig. 5, lane 1). Subunits of the complex migrate, largely according to their expected molecular mass, in the order: cytochrome *b* (420 aa plus the His_6-tag), cytochrome *c* (243 aa), the Rieske protein (210 aa), and the FbcX protein (160 aa). Next to a comprehensive mass spectroscopic analysis and N-terminal sequence information obtained for all four subunits (for details, see [35]), the cytochrome *c* subunit is easily visualized immunologically (Fig. 5, lane 2) using an antiserum directed against the hydrophilic *c*-domain; likewise, the His-tag introduced at the C-terminus of cytochrome *b* is identified (Fig. 5, lane 4).

Individual subunits of the *bc* complex and their fragments have been successfully expressed in and purified from *E. coli*, such as the heme *c* domain fragment (comprising the terminal 84 aa) used for antibody production, and the full-length cytochrome *c* carrying a C-terminal His-tag; for this purpose, host cells were cotransformed with pEC86 encoding the heme maturation factors [35,59].

Having proven the general feasibility of producing cofactor-containing *Thermus* proteins in *E. coli*, ([36], and see above), we set out to achieve expression of the complete *T. thermophilus fbc*CXFB operon in this heterologous host, thus

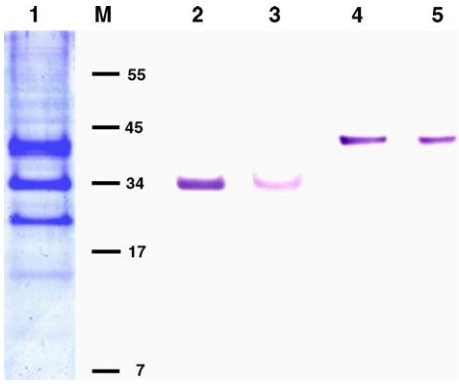

Fig. 5. Electrophoretic and immunological analysis of subunits of the isolated *T. thermophilus bc* complex. The purified complex after expression of the His-tagged operon in *T. thermophilus* (lanes 1, 2, and 4), or in *E. coli* (lanes 3 and 5) was electrophoresed on a Tricine gel (12% polyacrylamide) in the presence of SDS. Lane 1, Coomassie stained; lanes 2 and 3, Western blot using an antibody raised against the soluble *c*-heme domain; lanes 4 and 5, using an anti-his antibody. M: molecular weight marker (numbers in kDa). Cytochrome *b*: 420 aa, cytochrome *c*: 243 aa, Rieske protein: 210 aa, FbcX: 160 aa.

circumventing the necessity of constructing a *Thermus* strain deleted in *fbc* genes for later mutagenesis studies. Preliminary results confirm so far the synthesis of at least the *b* and *c* cytochrome subunits (see Fig. 5).

2.4. Redox cofactors characterized in the purified complex

Both cytochrome subunits are easily identified by visible redox spectroscopy. In an ascorbate-reduced minus oxidized difference spectrum of the entire *bc* complex, the absorbance for the *c*-type heme of the cytochrome *c* subunit is observed with a maximum at 555 nm and a shoulder at 548.5 nm; the dithionite-reduced minus oxidized redox spectrum, in addition, shows the absorption of the two *b*-type hemes with a maximum at 561.5 nm [35]. Based on pyridine-hemochrome spectra, molar absorption coefficients were calculated for cytochrome *c*: $\varepsilon_{555-620}=15.3\ mM^{-1}\ cm^{-1}$ and heme *b*: $\varepsilon_{561-620}=23.7\ mM^{-1}\ cm^{-1}$, yielding a stoichiometry of 1.7 (heme *b* to heme *c*) in the purified preparation.

Incorporation of the iron–sulfur cluster (2Fe·2S) is confirmed by EPR spectroscopy. In Fig. 6A, the *bc* complex is reduced with excess ascorbate (upper trace) and the rhombic EPR spectrum of a reduced iron–sulfur center is clearly seen. The *g*-tensor values are typical of those observed for a reduced Rieske FeS center. The position and lineshape of the observed g_{xx} value of 1.78 might suggest that the "putative" Q_o-site is occupied. There is no narrow signal observed at $g=2$, which would be typical of an organic radical, e.g., from a semiquinone anion. In the lower trace the sample has been reduced with dithionite and now in addition to the broad EPR signal from the Rieske center, an additional EPR signal at $g=2$ is observed. The overall linewidth and ^{1}H-ENDOR spectrum (data not shown) suggest that this signal most probably arises from a semiquinone formed at the Q_i site of the protein.

In a 2-D hyperfine sublevel correlation spectrum (HYSCORE), correlation cross peaks between hyperfine frequencies belonging to different M_s manifolds of the same nucleus can be observed [61]. The 2D HYSCORE spectrum of the Rieske center recorded at g_{zz} is presented as contour plot in Fig. 6B. Off-diagonal features are clearly observed. These double quantum-double quantum (dq–dq) correlation cross peaks (at 7.0, 3.6 MHz) are clearly resolved in the (+, −) quadrant of the HYSCORE spectrum (e.g., [62,63]) and are observed in all Rieske centers so far investigated in the literature using ESEEM/HYSCORE, clearly indicating the coordination of histidine to the iron–sulfur cluster.

Recently a detailed study of similar HYSCORE spectra [64] has suggested that they can be used to accurately resolve the geometry of the two coordinating histidines. Such a detailed analysis of the "low-potential" *T. thermophilus bc* Rieske center is currently underway in our lab.

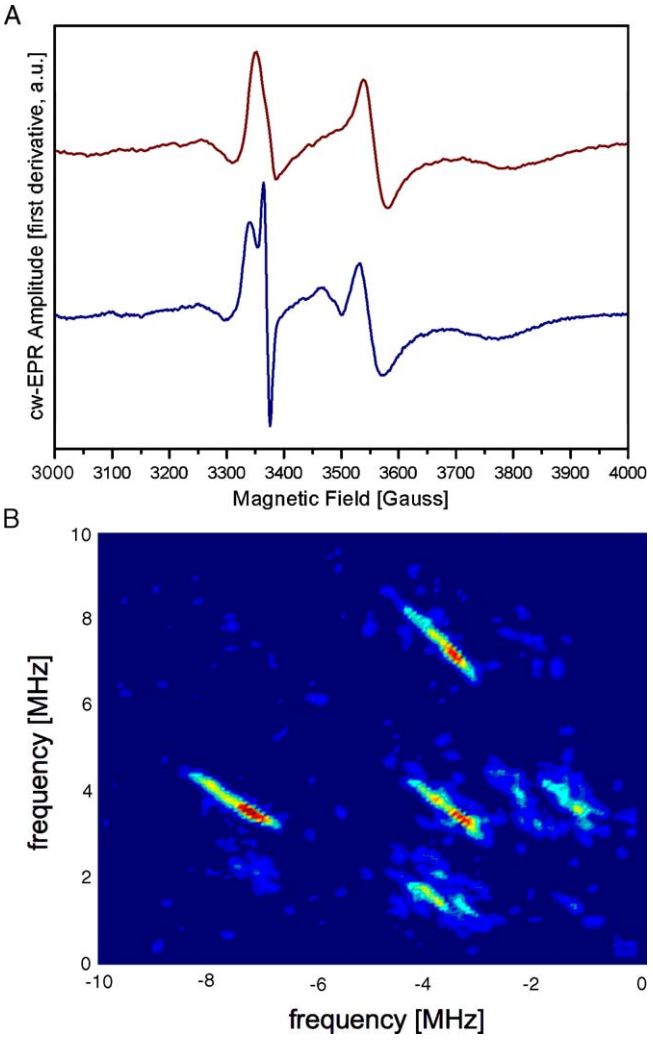

Fig. 6. Identification of the $Fe_2 \cdot S_2$ Rieske center in the isolated *T. thermophilus bc* complex. (A) cw-EPR spectra of the isolated *T. thermophilis bc* complex reduced with sodium ascorbate (upper trace) and with sodium dithionite (lower trace). Experimental conditions: microwave frequency: 9.44 GHz, microwave power, 1 mW; field modulation, 100 kHz; modulation amplitude ± 0.4 mT peak to peak, $T=20$K. (B) Fourier transformed HYSCORE spectrum of the *T. thermophilis bc* complex reduced with sodium dithionite. This 2-dimensional spectrum is recorded at low field canonical orientation of the Rieske signal ($g_{zz}=2.01$). Experimental conditions: τ; 120 ns; π/2 pulse length, 16 ns; π inversion pulse length, 32 ns, microwave frequency, 9.76 GHz; shot repetition time, 0.8 ms. For the 2D HYSCORE (π/2 − τ − π/2 − t_1 − π − t_2 − π/2 −τ − echo) spectrum a set of 256×256 data points was recorded where t_1 and t_2 were incremented in steps of 24 ns from their initial values. To remove the unwanted echoes, the appropriate 4-step phase-cycling procedures in the HYSCORE [60] experiment was applied. The background decay in both t_1 and t_2 dimensions was subtracted using a polynomial function followed by zero-filling to 512 points in both dimensions and tapering with a Hamming window. The 2D spectrum is shown in the absolute value mode.

2.5. Enzymatic activity and thermostability of the detergent-purified bc complex

With all cofactors obviously fully and correctly incorporated in the isolated 4-subunit *bc* complex, the isolated enzyme retains enzymatic activity. Measurements are hampered, however, by the fact that turnover activity tests have not yet been successfully performed at optimal temperature (see below), nor has a stable electron donor system been established. Menaquinol analogs, in combination with the native ET acceptor, *Thermus* c_{552}, proved too high in non-enzymatic oxidation rate. Our present standard activity system uses

ubiquinol (30 μM), and horse heart cytochrome *c* at 45 °C—far from the optimum *Thermus* growth temperature. Under these conditions a turnover rate of around 1 s^{-1} is observed. To confirm the specificity of this enzymatic reaction, equimolar amounts of different oxidized naphthoquinol derivatives added to the enzyme assay inhibit on a competitive level (data not shown).

To test for thermostability of the isolated *bc* complex in a detergent-solubilized state, the protein was incubated, at two different protein concentrations, for 10 min at temperatures up to 121 °C. The residual enzymatic activity was then determined under standard assay conditions at 45 °C, and compared to an untreated sample (Fig. 7A). The purified complex (reversibly) retains activity in detergent solution up to around 90 °C, but appears to be denatured at higher temperatures under these conditions.

A comparable result is observed for the isolated complex in detergent solution when, upon heating from 20 to 100 °C, conformational transitions in secondary structure elements are followed by CD spectroscopy. As the complete transition point appeared to exceed 100 °C, additions of 1 M and 2 M guanidinium hydrochloride, respectively, were made to decrease the denaturing temperature to below 100 °C. Under these conditions, the process was still not completed within the applicable temperature range, but higher concentrations of the denaturant proved unsuitable.

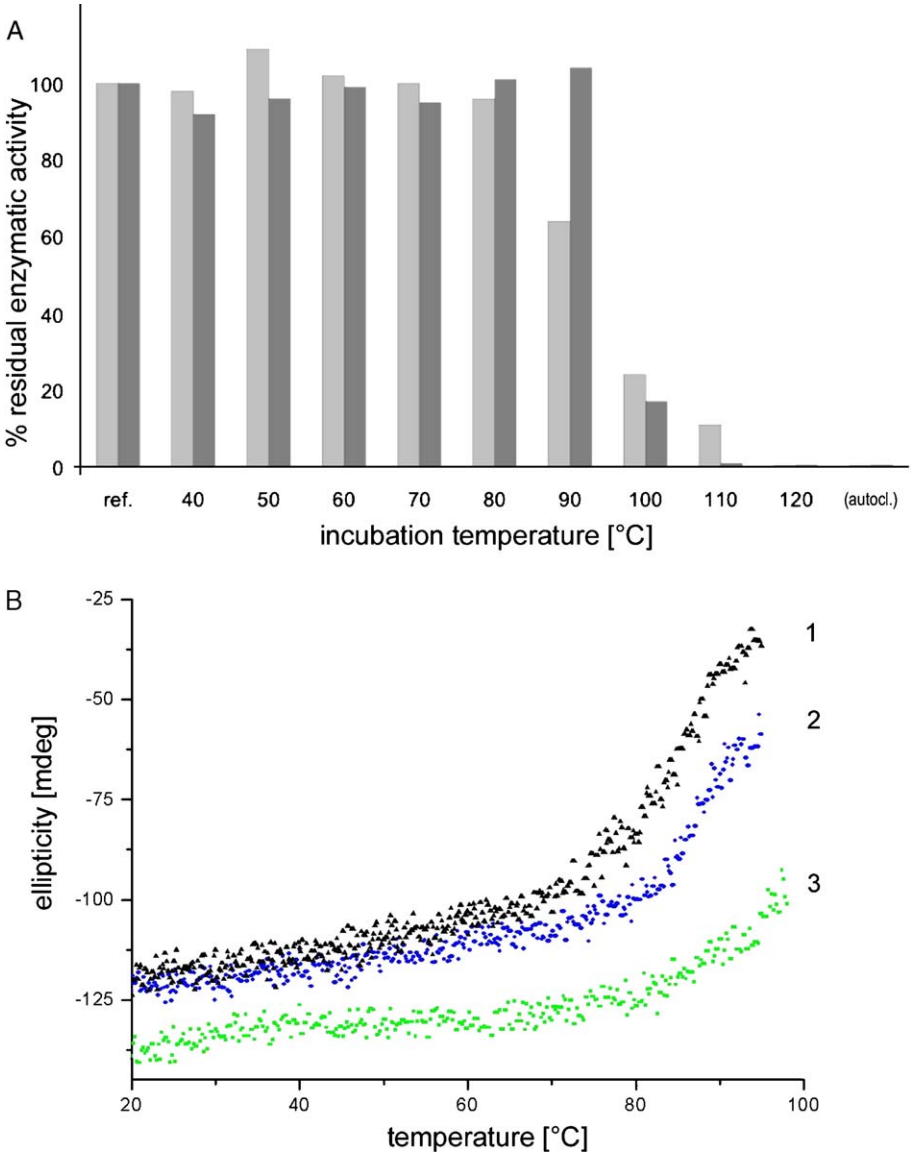

Fig. 7. Thermostability of the isolated *T. thermophilus bc* complex. (A) Residual enzymatic activity after incubation for 10 min at the given temperature in a sealed tube, of the isolated *bc* complex in 50 mM NaP_i, pH 7, 1.6 g/l decyl-maltoside, 150 mM NaCl and 10% glycerol; "autocl." refers to a standard autoclaving cycle with a holding time of 10 min. at 121 °C; "ref" is the 100% reference value omitting any heat treatment, corresponding to a turnover number of 1 s^{-1}. Light grey bars, enzyme incubated at a concentration of 9 μM; dark grey, at 90 μM. (B) CD spectra of the isolated *bc* complex without additives (3), with 1 M (2) and with 2 M guanidinium hydrochloride (1) in the temperature range of 20–95 °C. Spectra were recorded on a Jasco J-810 instrument, with the temperature range from 15 °C to 97 °C adjusted by a Jasco PTC 423S Peltier type temperature controller. The protein sample was diluted in buffer (50 mM NaP_i pH 7, 300 mM NaCl, 30% glycerol and 1.6 g/l decyl-maltoside) to a final concentration of 6 μM and CD spectra were obtained at a wavelength of 222 nm using a 1 mm path length cuvette.

2.6. Interaction of the bc complex with downstream redox partner in the T. thermophilus ET chain

In the respiratory chain of *T. thermophilus* the soluble cytochrome *c* is reduced by electrons from the *bc* complex. This reaction is one example of a specific interaction at very high reaction rates and thus requires an adapted mechanism for the recognition of the partner proteins.

To characterize this ET reaction, the interaction of the two proteins was investigated by stopped-flow spectroscopy. To simplify the experimental procedure an approach was chosen using the soluble domain of the cytochrome *c*, avoiding difficulties associated with membrane proteins; soluble domains have previously proven suitable models for ET reactions [25].

Very fast electron transfer rates of up to 2×10^7 and 1.7×10^7 M^{-1} s^{-1} for the forward (physiological) and reverse reactions were determined at low ionic strength for this reaction resulting in an equilibrium constant of about 1.1. The rate constants determined in the soluble system confirm that the two cytochromes are efficient reaction partners, and this notion should apply to the intact *bc* complex under physiological conditions in the membrane bilayer as well, even though steric restraints are higher than in the soluble fragments. Interestingly, the results of these experiments [35] indicate that the electron transfer rates are only slightly dependent on ionic strength, since the reaction partners interact with a $z_A z_B$ parameter of only −1.4 as calculated from the Brønsted plot of the data [35].

Comparing this finding with data from a related stopped-flow study using the *Thermus* cytochrome c_{552} and the soluble Cu_A domain of its ba_3 oxidase, an even lower contribution of charges in transient ET complex formation was observed [25]. Taking both sets of data together, it becomes obvious that interactions at elevated temperature are mainly governed by hydrophobic interactions, as noted also earlier [65], with only a minor electrostatic contribution.

3. Discussion

The identification of a functional *bc* complex has closed the gap in the aerobic respiratory chain of *Thermus thermophilus*, providing a central link between previously identified redox components involved in NADH and succinate oxidation, and the two well-known terminal oxidase branches. Beyond these basic properties, this four-subunit integral membrane protein complex addresses a number of further issues briefly summarized below.

3.1. The genomic organization mirrors the protein composition of the bc complex

Relying on early information from the *T. thermophilus* HB27 genome sequencing project (published in [5]), we took the Rieske fragment consensus motif to identify a locus of four consecutive genes apparently organized in a 3.1 kb operon-like structure (*fbc*CXFB, Fig. 2), notably characterized on the genetic level by a typical promoter region, a transcriptional terminator sequence, and the closely spaced coding regions for the structural genes. The last two of these open reading frames turned out to code bona fide subunits of canonical bc complexes, a cytochrome *b* and the full-length Rieske FeS subunit; the latter had been identified and characterized earlier in detail [36,37], though at that time studied without its N-terminal transmembrane anchor region. The first gene encoding a *c*-type cytochrome is expected as a complex III constituent as well, however its general protein topology, and the characteristics of its actual heme-binding domain as derived from sequence alignments (Figs. 2 and 3), make it highly unusual, see also below. The second gene in the operon structure encodes a hydrophobic polypeptide (Fig. 4) with almost no relationship with presently identified *bc* complexes.

When this *fbc*CXFB operon is expressed in *T. thermophilus*, in addition specifying a tag sequence at the C-terminus of the last gene product to allow for affinity purification [35], a complex consisting of all four gene products can be isolated, see Fig. 5. Thus, the subunit composition is a mirror image of the underlying operon structure. Care has to be taken, though, for the proper solubilization conditions, with best results obtained using decyl maltoside as the detergent, and glycerol for complex stabilization throughout; a subunit composition of the isolated complex of close to unity is obtained. It should be stressed that this pattern and the identity of subunits as observed on SDS gels is fully confirmed by extensive mass spectroscopy, by partial protein sequencing, and by immune-staining [35], establishing that all the operon-derived coding sequences and their respective protein modules as depicted in Fig. 2 are present as such in the four mature subunits in the complex.

3.2. A thermostable complex ...

With a maximum growth temperature for the organism of up to 85 °C, we expect a high degree of thermostability also for its proteins in a purified form; isolated membrane protein complexes are demanding also for the reason that they are deprived of their native membrane environment and surrounded by detergent micelles. Our approach to this question was twofold, and turned out to yield a fairly consistent result. The temperature profile for secondary structure changes was assayed by CD spectroscopy, and as a much more sensitive tool for structural desintegration, the irreversible loss of enzymatic activity was followed after a standard heat treatment of the isolated enzyme preparation. Both experimental criteria show a consistent protein stability of up to approx. 90 °C which collapses more or less abruptly at higher temperature values: while the first evidence for a structural perturbation is seen at around 80 °C in the CD data, irreversibly induced functional impairments become obvious at 90 °C, with some minor differences due to concentration effects (Fig. 7).

3.3. accepts electrons from menaquinol ...

The isolated protein complex is competent in enzymatic activity, but absolute turnover values obtained so far are fairly low (see Fig. 7A). A major obstacle is the high rate of (auto-) oxidation, already when measured at 45 °C, between menaquinol derivatives and the endogenous cytochrome c_{552}, and the

lack of suitable enzyme inhibitors. Using ubiquinol, not found in the ET chain of *Thermus* nor providing the suitable redox potential properties, a competition with (oxidized) MK compounds has been noted in the activity assay, pointing to the fact that the genuine substrate is indeed a naphthoquinol (data not shown). Little is known about the direct structural environment of such low-potential quinol binding sites, and with sufficient amounts of material now at hand, EPR spectroscopy should prove a valuable tool for future evaluations.

3.4. and uses unexpected protein modules ...

As outlined above, two of the four subunits of this thermophilic complex III are atyipcal and unexpected components. A sequence analysis links these two subunits to a *Deinococcus* gene product: a cytochrome c_6 protein appears to carry homologies to both subunit sequences, the cytochrome *c* subunit as well as the FbcX subunit of unknown function (Fig. 4), giving a first clue as to its evolutionary origin. Further mutagenesis and deletion studies will address the role, or necessity, of such extra protein domains or even subunits.

Even more surprising is the fact that the heme *c* binding domain of 86 aa of this complex III shares significant sequence homologies (Fig. 3) with a heme *c* domain of the caa_3-type terminal oxidases: there, on the C-terminal side of a regular Cu_A-liganding subunit II, a small cytochrome *c* is fused, presumably acting as a covalently attached substrate for these oxidases [19]. Unlike any canonical complex III where the heme *c* component is grouped either into the c_1- or *f*-type family, nature seems to have enjoyed picking a (any) different available module, similar to the *B. subtilis* situation (see Introduction), for an ET acceptor downstream of the cytochrome *b*/Rieske component complex (see also [4] for a more extended discussion on the evolution of complex III).

The obviously simultaneous usage of such a *c*-domain in any single organism is realized in *Thermus*, where next to the *bc* complex, a caa_3 terminal oxidase is found (see Introduction). This partial sequence identity does not show up in a standard multi-sequence comparison (as in Fig. 3A), but can be demonstrated for a pairwise alignment allowing several gaps; Fig. 3B (line 1 and 2) suggests stretches of sequence identity between both protein domains. Is it reasonable to find homologies in both domains, but not identity in sequence, and therefore in their 3-D structure? If a *bc* complex should interact directly with a terminal oxidase of the caa_3-type (see below), identity in the two most likely immediately interacting modules should be seriously counterproductive due to identical, and not complementary, surface properties; it will be interesting to verify, on structural grounds, this assumption in the future.

3.5. … to interact with two terminal oxidase branches

With the *bc* complex identified both on the genetic and protein level, this functional quinol reductase complements the previously established redox components in *T. thermophilus*, to yield a minimal respiratory chain operating under aerobic conditions (see Fig. 1). What interactions can be envisaged to supply electrons into both terminal oxidase branches? Using the 86 aa heme *c*-binding domain of the *bc* complex expressed in and purified from *E. coli*, an efficient redox interaction with cytochrome c_{552} has already been shown [35]: In accordance also with the subsequent ET step the soluble Cu_A fragment of the ba_3 oxidase (see Fig. 1, solid arrows; and [25]), the *c* / c_{552} redox couple displays little dependence on ionic strength. A careful appraisal of the kinetic data suggests only around one charge of opposite sign on each partner protein being responsible for the interaction. This situation once more points to the fact that protein contacts have evolved to rely less on ionic interactions as in mesophiles (see [25] for a specific example), but rather make use of hydrophobic interactions when optimized for elevated temperatures, as noted earlier [65].

How does the caa_3 oxidase receive electrons from complex III? With both complexes covalently carrying cytochrome *c* modules, a mitochondrial-type mobile cytochrome *c* shuffling electrons between complexes III and IV is not strictly required. Present evidence, again using soluble modules to study redox interactions (Julia Janzon et al., unpublished) supports this notion of a direct interaction between the two complexes. This leaves us with the interesting question as to whether both oxidase branches are specific and unique in their electron routing as discussed above, or whether the cytochrome c_{552} acts in a pool function (see Fig. 1) to supply electrons to both branches likewise. An experimental answer is expected from stopped-flow studies measuring ET reactions between the two partner modules, so far indicating an efficient interaction of the c_{552} with the *c*-domain of the caa_3 oxidase even at high ionic strength (F. Malatesta et al., unpublished data). As compared in Fig. 3B, protein sequences are highly related for the three *c*-domains from the *bc* complex, the caa_3 oxidase, and the c_{552} soluble cytochrome. In the light of this fact it will be interesting to learn how a mutual interaction between three such modules is feasible in terms of complementary interaction sites required for electron transfer.

Acknowledgments

We thank Wolfgang Nitschke, Marseille, for helpful discussions on complex III heme composition and classification, and Steffen Grimm, Frankfurt, for the CD measurements. We appreciate the hospitality of Maurizio Brunori, Rome, for using his stopped-flow apparatus, thank Oliver-Matthias H. Richter, Frankfurt, for discussions and critically reading the manuscript, and Hans-Werner Müller for excellent technical assistance. This work was funded in part by Hessisches Ministerium für Bildung und Wissenschaft and Deutsche Forschungsgemeinschaft (SFB 472); F. MacMillan acknowledges financial support from CMP (Center for Membrane Proteomics, Frankfurt).

References

[1] C. Vielle, G.J. Zeikus, Hyperthermophilic enzymes: sources, uses, and molecular mechanisms for thermostability, Microbiol. Mol. Biol. Rev. 65 (2001) 1–43.

[2] K.O. Stetter, Hyperthermophiles in the history of life, Ciba Found. Symp. 202 (1996) 1–10.
[3] M.V. Omelchenko, Y.I. Wolf, E.K. Gaidamakova, V.Y. Matosova, A. Vasilenko, M. Zhai, M.J. Daly, E.V. Koonin, K.S. Makarova, Comparative genomics of *Thermus thermophilus* and *Deinococcus radiodurans*: divergent routes of adaptation to thermophily and radiation resistance, BMC Evol. Biol. 5 (2005) 57–78.
[4] M. Schütz, M. Brugna, E. Lebrun, F. Baymann, R. Huber, K.O. Stetter, G. Hauska, R. Toci, D. Lemesle-Meunier, P. Tron, C. Schmidt, W. Nitschke, Early evolution of cytochrome *bc* complexes, J. Mol. Biol. 300 (2000) 663–675.
[5] A. Henne, H. Bruggemann, C. Raasch, A. Wiezer, T. Hartsch, H. Liesegang, A. Johann, T. Lienard, O. Gohl, R. Martinez-Arias, C. Jacobi, V. Starkuviene, S. Schlenczeck, S. Dencker, R. Huber, H.P. Klenk, W. Kramer, R. Merkl, G. Gottschalk, H.J. Fritz, The genome sequence of the extreme thermophile *Thermus thermophilus*, Nat. Biotechnol. 22 (2004) 547–553.
[6] R. Masui, K. Kurokawa, N. Nakagawa, F. Tokunaga, Y. Koyama, T. Shibata, T. Oshima, S. Yokoyama, T. Yasunaga, S. Kuramitsu, Complete genome sequence of Thermus thermophilus HB8, NCBI http://www.ncbi.nlm.nih.gov/gquery/gquery.fcgi?term=thermus+hb8.
[7] R. Moreno, A. Haro, A. Castellanos, J. Berenguer, High-level overproduction of his-tagged *Tth* DNA polymerase in *Thermus thermophilus*, Appl. Environ. Microbiol. 71 (2005) 591–593.
[8] R.A. Bernal, D. Stock, Three-dimensional structure of the intact *Thermus thermophilus* H^+-ATPase/synthase by electron microscopy, Structure 12 (2004) 1789–1798.
[9] S. Petry, D.E. Brodersen, F.V. Murphy, C.M. Dunham, M. Selmer, M.J. Tarry, A.C. Kelley, V. Ramakrishnan, Crystal structure of the ribosome in complex with release factors RF1 and RF2 bound to a cognate stop codon, Cell 123 (2005) 1255–1266.
[10] A. McKay, J. Quilter, C.W. Jones, Energy conservation in the extreme thermophile *Thermus thermophilus* HB8, Arch. Microbiol. 131 (1982) 43–50.
[11] M.D. Collins, H.N. Shah, D.E. Minnikin, A note on the separation of natural mixtures of bacterial menaquinones using reverse phase thin-layer chromatography, J. Appl. Bacteriol. 48 (1980) 277–282.
[12] J.A. Fee, M.G. Choc, K.L. Findling, R. Lorence, T. Yoshida, Properties of a copper-containing cytochrome c_1aa_3 complex: a terminal oxidase of the extreme thermophile *Thermus thermophilus* HB8, Proc. Natl. Acad. Sci. U. S. A. 77 (1980) 147–151.
[13] K. Hon-nami, T. Oshima, Cytochrome oxidase from an extreme thermophile, *Thermus thermohilus* HB8, Biochem. Biophys. Res. Commun. 92 (1980) 1023–1029.
[14] K. Hon-nami, T. Oshima, Purification and characterization of cytochrome *c* oxidase from *Thermus thermophilus* HB8, Biochemistry 23 (1984) 454–460.
[15] T. Yoshida, J.A. Fee, Studies on cytochrome *c* oxidase activity of the cytochrome c_1aa_3 complex from *Thermus thermophilus*, J. Biol. Chem. 259 (1984) 1031–1036.
[16] G. Buse, S. Hensel, J.A. Fee, Evidence for cytochrome oxidase subunit I and a cytochrome *c*-subunit II fused protein in the cytochrome 'c_1aa_3' of *Thermus thermophilus*, Eur. J. Biochem. 191 (1989) 261–268.
[17] B.H. Zimmermann, C.I. Nitsche, J.A. Fee, F. Rusnak, E. Munck, Properties of a copper-containing cytochrome ba_3: a second terminal oxidase from the extreme thermophile *Thermus thermophilus*, Proc. Natl. Acad. Sci. U. S. A. 85 (1988) 5779–5783.
[18] T. Soulimane, G. Buse, G.P. Bourenkov, H.D. Bartunik, R. Huber, M.E. Than, Structure and mechanism of the aberrant ba_3-cytochrome *c* oxidase from *Thermus thermophilus*, EMBO J. 19 (2000) 1766–1776.
[19] M.M. Pereira, M. Santana, M. Teixeira, A novel scenario for the evolution of haem-copper oxygen reductases, Biochim. Biophys. Acta 1505 (2001) 185–208.
[20] A. Kannt, T. Soulimane, G. Buse, A. Becker, E. Bamberg, H. Michel, Electrical current generation and proton pumping catalyzed by the ba_3-type cytochrome *c* oxidase from *Thermus thermophilus*, FEBS Lett. 434 (1998) 17–22.
[21] K. Hon-Nami, T. Oshima, Purification and some properties of cytochrome c_{552} from an extreme thermophile, *Thermus thermophilus* HB8, J. Biochem. (Tokyo) 82 (1977) 769–776.
[22] M.E. Than, P. Hof, R. Huber, G..P. Bourenkov, H.D. Bartunik, G. Buse, T. Soulimane, *Thermus thermophilus* cytochrome-c_{552}: a new highly thermostable cytochrome-*c* structure obtained by MAD phasing, J. Mol. Biol. 271 (1997) 629–644.
[23] T. Soulimane, M. von Walter, P. Hof, M.E. Than, R. Huber, G. Buse, Cytochrome-c_{552} from *Thermus thermophilus*: a functional and crystallographic investigation, Biochem. Biophys. Res. Commun. 237 (1997) 572–576.
[24] P.A. Williams, N.J. Blackburn, D. Sanders, H. Bellamy, E.A. Stura, J.A. Fee, D.E. McRee, The Cu_A domain of *Thermus thermophilus* ba_3-type cytochrome *c* oxidase at 1.6 Å resolution, Nat. Struct. Biol. 6 (1999) 509–516.
[25] O. Maneg, B. Ludwig, F. Malatesta, Different interaction modes of two cytochrome-*c* oxidase soluble Cu_A fragments with their substrates, J. Biol. Chem. 278 (2003) 46734–46740.
[26] O. Maneg, F. Malatesta, B. Ludwig, V. Drosou, Interaction of cytochrome *c* with cytochrome oxidase: two different docking scenarios, Biochim. Biophys. Acta 1655 (2004) 274–281.
[27] T. Yagi, K. Hon-Nami, T. Ohnishi, Purification and characterization of two types of NADH-quinone reductase from *Thermus thermophilus* HB-8, Biochemistry 27 (1988) 2008–2013.
[28] T. Yano, S.S. Chu, V.D. Sled', T. Ohnishi, T. Yagi, The proton-translocating NADH-quinone oxidoreductase (NDH-1) of thermophilic bacterium *Thermus thermophilus* HB-8. Complete DNA sequence of the gene cluster and thermostable properties of the expressed NQO2 subunit, J. Biol. Chem. 272 (1997) 4201–4211.
[29] P. Hinchliffe, L.A. Sazanov, Organization of iron–sulfur clusters in respiratory complex I, Science 309 (2005) 771–774.
[30] L.A. Sazanov, P. Hinchliffe, Structure of the hydrophilic domain of respiratory complex I from *Thermus thermophilus*, Science 311 (2006) 1430–1436.
[31] H.-J. Park, C.O.A. Reiser, S. Kondruweit, H. Erdamnn, R.D. Schmid, M. Sprinzl, Purification and characterization of a NADH oxidase from the thermophile *Thermus thermophilus* HB8, Eur. J. Biochem. 205 (1992) 881–885.
[32] M. Stupak, G. Zoldak, A. Musatov, M. Sprinzl, E. Sedlak, Unusual effect of salts on the homodimeric structure of NADH oxidase from *Thermus thermophilus* in acidic pH, Biochim. Biophys. Acta 1764 (2006) 129–137.
[33] T. Soulimane, G. Buse, Conference Abstract, GBM-Meeting Hamburg, Germany, 1999.
[34] F. Cava, J. Berenguer, Biochemical and regulatory properties of a respiratory island encoded by a conjugative plasmid in the extreme thermophile *Thermus thermophilus*, Biochem. Soc. Trans. 34 (2005) 97–100.
[35] D. Mooser, O. Maneg, C. Corvey, T. Steiner, F. Malatesta, M. Karas, T. Soulimane, B. Ludwig, A four-subunit cytochrome bc_1 complex complements the respiratory chain of *Thermus thermophilus*, Biochim. Biophys. Acta 1708 (2005) 262–274.
[36] J.A. Fee, K.L. Findling, T. Yoshida, R. Hille, G.E. Tarr, D.O. Hearshen, W.R. Dunham, E.P. Day, T.A. Kent, E. Munck, Purification and characterization of the Rieske iron–sulfur protein from *Thermus thermophilus*. Evidence for a [2Fe–2S] cluster having non-cysteine ligands, J. Biol. Chem. 259 (1984) 124–133.
[37] L.M. Hunsicker-Wang, A. Heine, Y. Chen, E.P. Luna, T. Todaro, Y.M. Zhang, P.A. Williams, D.E. McRee, J. Hirst, C.D. Stout, J.A. Fee, High-resolution structure of the soluble, respiratory-type Rieske protein from *Thermus thermophilus*: analysis and comparison, Biochemistry 42 (2003) 7303–7317.
[38] Y. Zu, J.A. Fee, J. Hirst, Complete thermodynamic characterization of reduction and protonation of the $bc_{(1)}$-type Rieske [2Fe–2S] center of *Thermus thermophilus*, J. Am. Chem. Soc. 123 (2001) 9906–9907.
[39] D.L. Gatti, G. Tarr, J.A. Fee, S.H. Ackerman, Cloning and sequence analysis of the structural gene for the bc_1-type Rieske iron–sulfur protein from *Thermus thermophilus* HB8, J. Bioenerg. Biomembranes 30 (1998) 223–233.
[40] E.A. Berry, M. Guergova-Kuras, L.-S. Huang, A.R. Crofts, Structure and

function of cytochrome *bc* complexes, Annu. Rev. Biochem. 69 (2000) 1005–1075.
[41] E. Darrouzet, J.W. Cooley, F. Daldal, The cytochrome bc_1 complex and its homologue the b_6f complex: similarities and differences, Photosynth. Res. 79 (2004) 25–44.
[42] M.M. Pereira, T.M. Bandeiras, A.S. Fernandes, R.S. Lemos, A.M.P. Melo, M. Teixeira, Respiratory chains from aerobic thermophilic prokaryotes, J. Bioenerg. Biomembr. 36 (2004) 93–105.
[43] M. Schütz, B. Schoepp-Cothenet, E. Lojou, M. Woodsta, D. Lexa, P. Tron, A. Dolla, M.C. Stetter, F. Baymann, The naphthoquinol oxidizing cytochrome bc_1 complex of the hyperthermophilic knallgasbacterium *Aquifex aeolicus*: properties and phylogenetic relationships, Biochemistry 16 ((36) 42) (2003) 10800–10808.
[44] E. Kutoh, N. Sone, Quinol-cytochrome c oxidoreductase from the thermophilic bacterium PS3, J. Biol. Chem. 263 (1988) 9020–9026.
[45] U. Liebl, S. Pezennec, A. Riedel, E. Kellner, W. Nitschke, The Rieske FeS center from the gram-positive bacterium PS3 and its interaction with the menaquinone pool studied by EPR, J. Biol. Chem. 267 (1992) 14068–14072.
[46] J. Yu, L. Hederstedt, P.J. Piggot, The cytochrome *bc* complex (Menaquinone:Cytochrome *c* Reductase) in *Bacillus subtilis* has a nontraditional subunit organization, J. Bacteriol. 177 (1995) 6751–6760.
[47] M. Bott, A. Niebisch, The respiratory chain of *Corynebacterium glutamicum*, J. Biotechnol. 104 (2003) 129–153.
[48] N. Sone, M. Fukuda, S. Katayama, A. Jyoudai, M. Syugyou, S. Noguchi, J. Sakamoto, *QcrCAB* operon of a nocardia-form actinomycete *Rhodococcus rhodochrous* encodes cytochrome reductase, Biochim. Biophys. Acta 1557 (2003) 125–131.
[49] M.M. Pereira, J.N. Carita, M. Teixeira, Membrane-bound electron transfer chain of the thermohalophilic bacterium *Rhodothermus marinus*: a novel multihemic cytochrome *bc*, a new complex III, Biochemistry 38 (1999) 1268–1275.
[50] S.F. Altschul, T.L. Madden, A.A. Schaffer, J. Zhang, Z. Zhang, W. Miller, D.J. Lipman, Gapped BLAST and PSI-BLAST: a new generation of protein database search programs, Nucleic Acids Res. 25 (1997) 3389–3402.
[51] M. Cserzo, E. Wallin, I. Simon, G. von Heijne, A. Elofsson, Prediction of transmembrane alpha-helices in prokaryotic membrane proteins: the dense alignment surface method, Protein Eng. 10 (1997) 673–676.
[52] G.R. Moore, G.W. Pettigrew, Axial ligation of cytochrome f and cytochrome c_1, Cytochromes c, Evolutionary, Structural and Physicochemical Aspects, Springer-Verlag, Berlin, 1990, pp. 66–71.
[53] W.R. Pearson, Rapid and sensitive sequence comparison with FASTP and FASTA, Methods Enzymol. 183 (1990) 63–98.
[54] M.G. Claros, G. von Heijne, TopPred II: an improved software for membrane protein structure predictions, CABIOS 10 (1994) 685–686.
[55] O. White, J.A. Eisen, J.F. Heidelberg, E.K. Hickey, J.D. Peterson, R.J. Dodson, D.H. Haft, M.L. Gwinn, W.C. Nelson, D.L. Richardson, K.S. Moffat, H. Qin, L. Jiang, W. Pamphile, M. Crosby, M. Shen, J.J. Vamathevan, P. Lam, L. McDonald, T. Utterback, C. Zalewski, K.S. Makarova, L. Aravind, M.J. Daly, K.W. Minton, R.D. Fleischmann, K.A. Ketchum, K.E. Nelson, S. Salzberg, H.O. Smith, J.C. Venter, C.M. Fraser, Genome sequence of the radioresistant bacterium *Deinococcus radiodurans* R1, Science 286 (1999) 1571–1577.
[56] NCBI: *Deinococcus geothermalis* DSM 11300, unfinished sequence, whole genome shotgun sequencing project. http://www.ncbi.nlm.nih.gov/entrez/query.fcgi?db=genome_and_cmd=search_and_term=deinococcus+geothermalis.
[57] B.C. Berks, T. Palmer, F. Sargent, Protein targeting by the bacterial twin-arginine translocation (Tat) pathway, Curr. Opin. Microbiol. 8 (2005) 174–181.
[58] D. Stroebel, Y. Choquet, J.L. Popot, D. Picot, An atypical heam in the cytochrome b(6)f complex, Nature 426 (2003) 399–400.
[59] E. Arslan, H. Schulz, R. Zufferey, P. Kunzler, L. Thony-Meyer, Overproduction of the *Bradyrhizobium japonicum c*-type cytochrome subunits of the cbb_3 oxidase in *Escherichia coli*, Biochem. Biophys. Res. Commun. 251 (1998) 744–747.
[60] G. Gemperle, G. Aebli, A. Schweiger, R.R. Ernst, Phase cycling in pulse EPR, J. Magn. Reson. 88 (1990) 241–256.
[61] P. Höfer, A. Grupp, H. Nebenführ, M. Mehring, Hyperfine sublevel correlation (Hyscore) spectroscopy-a 2d electron-spin-resonance investigation of the squaric acid radical, Chem. Phys. Lett. 132 (1986) 279–282.
[62] R.D. Britt, K. Sauer, M.P. Klein, D.B. Knaff, A. Kriauciunas, C.-A. Yu, L. Yu, R. Malkin, Electron spin echo envelope modulation spectroscopy supports the suggested coordination of two histidine ligands to the Rieske Fe–S centers of the cytochrome b6f complex of spinach and the cytochrome bc_1 complexes of *Rhodospirillum rubrum*, *Rhodobacter sphaeroides* R-26, and bovine heart mitochondria, Biochemistry 30 (1991) 1892–1901.
[63] S.A. Dikanov, L. Xun, A.B. Karpiel, A.M. Tyryshkin, M.K. Bowman, Orientationally-selected two-dimensional ESEEM spectroscopy of the Rieske-type iron–sulfur cluster in 2,4,5-trichlorophenoxyacetate monooxygenase from *Burkholderia cepacia* AC1100, JACS 118 (1996) 8408–8416.
[64] S.A. Dikanov, A.A. Shubin, A. Kounosu, T. Iwasaki, R.I. Samioilova, A comparative, two-dimensional N-14 ESEEM characterization of reduced [2Fe–2S] clusters in hyperthermophilic archaeal high- and low-potential Rieske-type proteins, JBIC 9 (2004) 753–767.
[65] A. Giuffrè, E. Forte, G. Antonini, E. D'Itri, M. Brunori, T. Soulimane, G. Buse, Kinetic properties of ba_3 oxidase from *Thermus thermophilus*: effect of temperature, Biochemistry 38 (1999) 1057–1065.